

Geological carbon storage: processes, risks and opportunities

Holger Ott, Imperial College, Shell Global Solutions International B.V

ABSTRACT

Due to the growing global demand for energy and the relatively slow transition to sustainable energy sources, the combustion of carbon-based fuels will remain the world's major energy source for the coming decades. In order to achieve climate targets, transition technologies are required to reduce CO₂ emissions during this period. Carbon Capture and Storage (CCS) is such a technology with a high potential to reduce greenhouse-gas emissions, and potentially even achieve a negative CO₂ footprint – i.e. an active transfer of CO₂ into the long-term carbon cycle. While for CO₂ capture and transport, cost efficiency is the main issue, subsurface storage is focused on storage capacity and storage safety. With this in mind, CCS is discussed in relation to energy demand, anthropogenic CO₂ emissions and 'clean fossil fuels'. The main focus is on CO₂ storage in geological formations. CO₂ migration and trapping mechanisms in deep saline aquifers and depleted hydrocarbon reservoirs are discussed and related to performance and risk assessment of injection operations. Finally, a glance on current subsurface research and development is given.

INTRODUCTION

The Challenge

Currently, more than 80% of the world's primary energy supply is based on fossil fuels, i.e. on the combustion of coal, oil, and gas. There are two major issues in conjunction with fossil fuel combustion. First, the earth's fossil fuel reserves accessible for economical extraction are finite, with a currently estimated remainder of ~110 years for coal, ~50 years for oil, ~60 years for natural gas, on the basis of the present day's level of energy consumption in the future [EIA, 2014] – a scenario that is not very likely in view of the current growth rate of the total energy consumption. Second, the combustion of fossil fuels releases carbon dioxide and is to a large extent responsible for the increase of the atmospheric CO₂ concentrations [IPCC, 2005]. It has been estimated that fossil fuels account for about 75% of the current anthropogenic CO₂ emissions [IPCC, 2005]. There is a general understanding that the current level of CO₂ emissions is unsustainable and that a key element for greenhouse gas reduction is linked to primary energy production. Thus, energy industries and public organizations simulate future energy scenarios based on statistical data and including different future energy policies to understand and predict future developments of the energy market.

The left image of Fig. 1 shows the result of an energy scenario considered by Shell. There are two obvious trends: firstly, the overall energy demand is increasing in the period up to 2050, and secondly, the total demand for fossil fuels will reach a maximum – at around 2040 in the Shell scenario – and declines thereafter, while alternative forms of energy increase in their importance. However, despite this trend, the share of fossil fuels is predicted to still be very high in 2050, decreasing from above 80% today to about 70% in 2050. Different mitigation scenarios considered by the Intergovernmental Panel on Climate Change still predict a share of fossil fuels of well above 50% by 2100 as shown in the right image of Fig. 1. A high share of fossil fuels in the energy mix is a characteristic of the energy scenarios of different organizations [Shell, 2013; IEA, 2014; IPCC, 2014] and reflects the inertia in the energy market with respect to existing infrastructure and investments. This is important to recognize,

since the speed of restructuring the energy sector is not necessarily determined by the speed of technology development of e.g. alternative energy technologies, but rather by the inertia of the energy system caused by capacity, existing plants and infrastructure versus investment in new technology and in distribution networks.

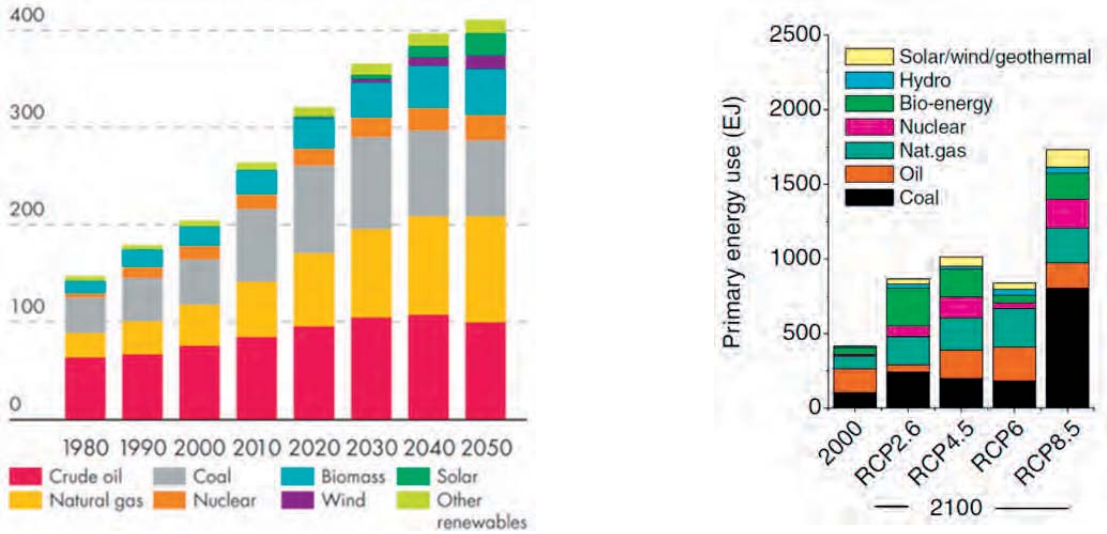


Figure 1: Left: energy scenario considered by Shell. Vertical axis: primary energy demand in units of million barrels of oil equivalent per day (MMBOED). 400 MMBOED correspond to about 858 EJ/a. The compositions is given as color coding. Right: predicted energy mixes for the year 2100 as results of climate models with different representative concentration pathways (RCP) compared to the energy mix in the year 2000. The four RCPs, RCP2.6, RCP4.5, RCP6, and RCP8.5, are named after a possible range of radiative forcing values in the year 2100 relative to pre-industrial values (+2.6, +4.5, +6.0, and +8.5 W/m², respectively) [IPCC, 2014; van Vuuren, 2011].

In conclusion, in addition to a strong emphasis on developing a renewable-energy future, the challenge of mitigating consequences of fossil fuel consumption over the coming decades must also be addressed.

Driving Forces for CCS

Carbon Capture and Storage (CCS) could play a vital role in mitigating greenhouse gas emissions to the atmosphere. When CCS first became a topic of interest in the 1990s, it was considered to be a technology that (1) was transitional, (2) could be deployed quicker than renewables, and (3) would be cheaper than renewables. As time progressed, CCS has been seen in a different light. In modern energy scenarios CCS appears as technology that can be combined with central biomass combustion or gasification to provide negative-CO₂ pathways to create a negative offset for continued use of oil and gas in sectors where this is hard to replace. Secondly, pre-combustion capture that produces hydrogen that can be flexibly used for low-carbon power generation becomes a key enabler at the system level.

The combination of CCS and biomass combustion (BECCS) has the potential to actively reduce the atmospheric CO₂ concentration [Benson, 2014]. Demanding mitigation scenarios aim for atmospheric concentrations of 450 to 550 ppm CO₂eq (CO₂ equivalent) in 2100, with a temporary overshoot. Overshooting scenarios – in contrast to long-term accumulating scenarios – typically rely on the widespread deployment of BECCS and afforestation in the second half of the century [IPCC, 2014]. The availability and scale of CCS, BECCS, and

other mitigation technologies are uncertain and are associated with several challenges and risks. However, many climate models could not achieve atmospheric concentration levels of about 450 ppm CO₂eq in the absence, only limited availability or delayed deployment of key technologies, such as bioenergy, CCS, and their combination (BECCS) [IPCC, 2014].

The magnitude of required emission reduction is large. It has been shown that the cumulative carbon emission between 2011 and 2050 needs to be limited to 1100 Gt of CO₂ in order to limit global warming to 2°C throughout the 21st century [Meinshausen, 2009; McGlade, 2015]. The present estimates of the global fossil fuel resources contain ~3× more carbon emissions potential [Raupach, 2014; McGlade, 2015], corresponding to ~3300 Gt of CO₂. In comparison the total ongoing and currently projected CCS operations add up to only 9.1 Gt in total up to 2100 [Global CCS Institute, 2015]. This indicates that the current efforts clearly are by far not yet adequate.

Carbon Capture and Storage (CCS)

CCS describes a set of technologies for separating CO₂ from the exhaust of large emitters and storing it below the surface over geological time scales. Only large point sources allow for effective CO₂ capture and transport with currently available technologies. Typical point sources are fossil-fueled power plants and other CO₂-intensive industries such as the cement and the steel industry [MIT, 2015]. CCS is also a key enabler for the upstream industry, when large amounts of CO₂ are produced in hydrocarbon production operations and a disposal concept is required.

There are different pathways for carbon capture depending on the nature of the emitter. The most common one is the so-called post-combustion capture technology that separates CO₂ from the exhaust stream after combustion. The advantage of this is that post-combustion capture is an add-on technology, with which existing plants or works can be retrofitted. More sophisticated techniques are available, which are part of the process and hence part of the plant or work. The most common ones are pre-combustion capture and oxyfuel combustion. Current developments are focused on the reduction of the costs for power generation with CCS which are still a factor of ~1.5 to 2 times the costs without CCS [IPCC, 2005], and, associated to this, reduction of the energy demand (15–30% of the generated power), and optimization of integration with power generation processes or other applications.

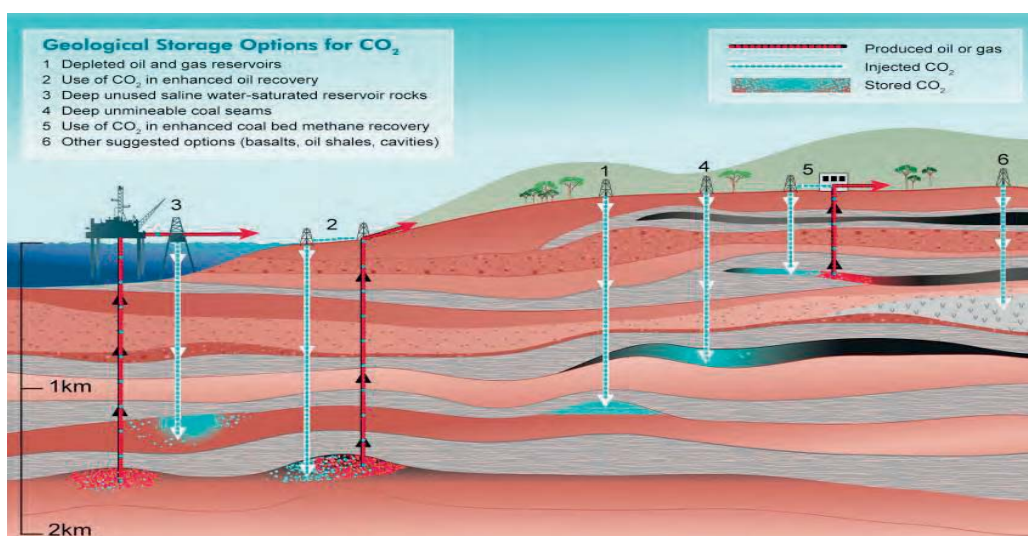


Figure 2: The various reservoirs for geological storage of CO₂ [IPCC, 2005].

The pure and compressed CO₂ stream can be transported via pipelines – and in exceptional cases by vessels – to the storage site. While cost efficiency is the main issue for CO₂ capture and transport, subsurface storage is focused on storage capacity, performance, and safety. There are many suitable types of reservoir: CO₂ can be stored in geological formations including oil and gas reservoirs, unmineable coal seams, and deep saline formations. When selecting a reservoir, there are several aspects to be considered: (1) the reservoir should be in proximity to the point source, (2) the storage capacity and the injectivity should allow a high injection rate over the lifetime of the emitting plant, and (3) the reservoir must be well characterized and the injection and storage processes must be well understood to ensure safe storage.

The storage options are schematically shown in Fig. 2. Currently, the most promising geological reservoirs are depleted hydrocarbon fields and deep saline aquifers. Depleted fields are usually well characterized and have proven seals. Also, the infrastructure such as injection wells and pipelines are already in place, which might reduce costs. In the ideal case, CCS can be combined with hydrocarbon production. CO₂ has been injected for enhanced oil recovery [Lake, 1989] or enhanced coalbed methane (ECBM) recovery [Busch, 2011]. However, CO₂ utilization for hydrocarbon recovery is likely to remain a niche given the volume of CO₂ required to be sequestered. Saline aquifers, on the other hand, are generally more abundant – therefore more likely to be found in proximity to a point source – and should offer a much higher total storage capacity.

SUBSURFACE PROCESSES

For geological storage, CO₂ is injected into porous (sedimentary) rock formations deep underground. The fluids in these deep formations are at high pressure and temperature conditions (corresponding to hydrostatic pressure and geothermal gradients of typically ~100 bar (10⁷ Pa) and ~30°C increase per km depth, respectively, however, for many reservoirs deviations from these rules occur).

Primary Displacement Processes: To penetrate a formation, CO₂ must be injected at a higher pressure than the initial fluid pressure in order to displace the fluids that are initially in place.

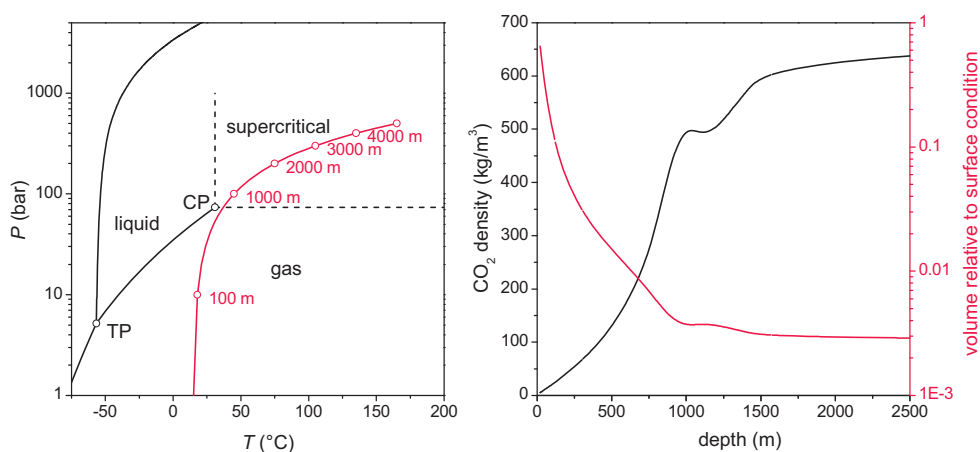


Figure 3: Left: CO₂ phase diagram as a function of pressure and temperature. The red line indicates the pressure and temperature conditions assuming a normal geothermal gradient and hydrostatic pressure as reservoir pressure. TP denotes the triple point and CP the critical point. Right: CO₂ density as a function of depth and the CO₂ volume relative to the volume at surface conditions (1 bar, 15 °C).

The target reservoirs are usually at a depth of more than 800 m, because assuming the pressure and temperature gradients discussed above, CO₂ is supercritical at these depths, as indicated in Fig. 3. Supercritical CO₂ (scCO₂) is beneficial for CO₂ storage; it has the viscosity of a gas but a density of a liquid which combines the advantages of a lower pressure response during injection with a high utilization of storage capacity in a given pore space – a high pore-space utilization. However, the density of CO₂ under reservoir conditions is still smaller than the density of the brine initially occupying the pore space, causing the CO₂ to migrate upward by buoyancy. Disregarding the special case of pure hydrodynamic trapping that does not require an upper seal as suggested by [Bachu, 1994], a sealing layer above the reservoir is therefore generally required to prevent CO₂ leaking to higher formations (e.g. drinking-water aquifers) or to the surface,.

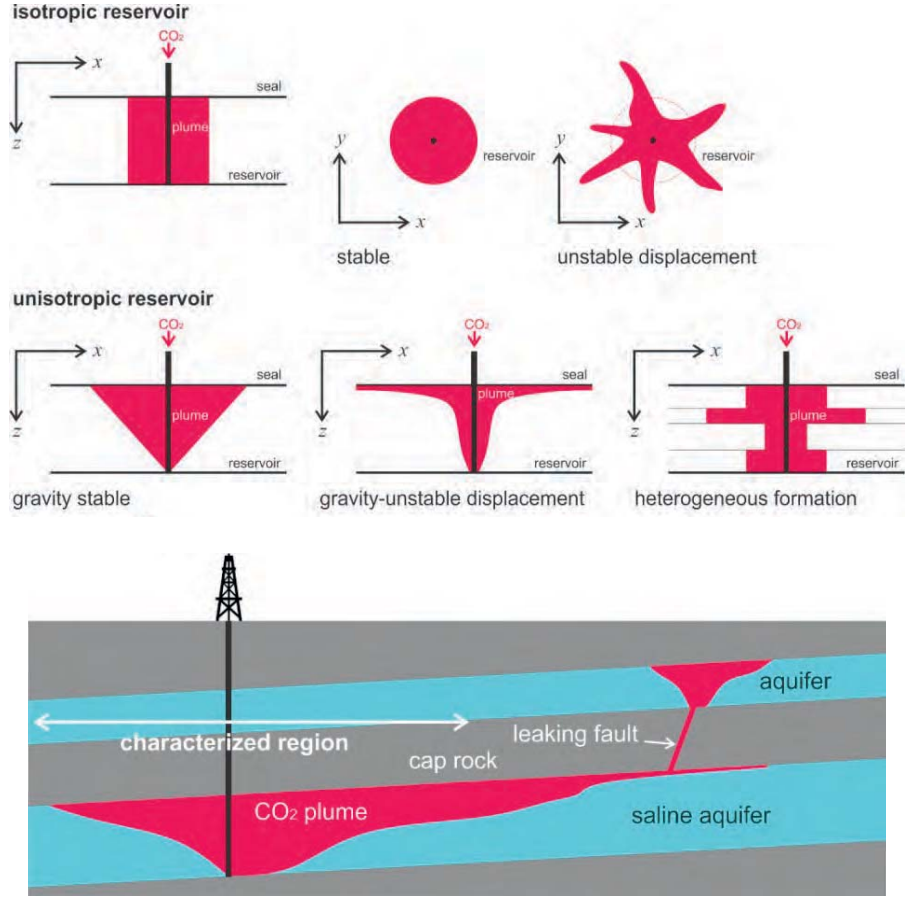


Figure 4: Upper images: schematic of primary plume migration and effects of gravity, fluid mobility ratio and heterogeneity on sweep efficiency and plume shape. Lower image: plume migration in a dipping reservoir and potential leakage pathway away from the characterized zone.

There is no “typical architecture” of a reservoir. However, an illustrative example is an anticlinal structure with a series of permeable and impermeable layers, where the permeable layers could serve as CO₂ storage or CO₂ reservoirs and a series of impermeable layers on top would form the seal. Typically, shales or salt layers (evaporates) with sufficient thickness (100s of meters) and quality are considered as acceptable seals. Such layers are not strictly impermeable, but their permeability is many orders of magnitude smaller than the permeability of the reservoir (nano Darcy vs. Darcy or 10⁻²¹ vs. 10⁻¹² m²), such that migration through a seal of reasonable thickness requires geological time scales. Characteristic

properties of the seal layers are their capillary entry pressure, above which non-wetting CO₂ may enter the otherwise water-saturated seal (for shales), and the so-called fracturing pressure above which the seal becomes fractured and potentially leaky. Both pressures, with a safety margin, limit the injection pressure.

CO₂ and water (or brine) are mutually soluble but immiscible and hence CO₂-brine displacement is subject to two-phase (general multi-phase) flow. In contrast to the injection of a miscible fluid, immiscible displacement is never complete, i.e. just a fraction of the pore space is invaded by CO₂. In reservoir engineering this is called the microscopic displacement efficiency and for a practical purpose this is described by Darcy's law (extended to two-phase flow) including relative-permeability and capillary-pressure saturation functions. In simple cases, the saturation profiles and the microscopic displacement efficiency can be derived analytically [Buckley and Leverett, 1942; Lake, 1989].

On a macroscopic scale, i.e. field scale, the displacement efficiency is hampered by gravity, leading to a gravity-driven override of the CO₂ and hence bypassing of the pore space in the lower part of the reservoir. Also rock heterogeneity, i.e. layering, and viscous instabilities can lead to channeling and fingering, with the result that rock matrix is macroscopically bypassed. These situations are sketched in Fig. 4. The total pore space utilized for CO₂ storage, ϕ_U , can be computed from the porosity ϕ , the displacement efficiency ED and the volumetric sweep efficiency, EV , by $\phi_U = \phi \cdot ED \cdot EV$, with the range of ED and EV being between 0 and 1. It becomes obvious that only a fraction of the pore space is actually used for storage of scCO₂. This has consequences: (1) with a low pore space utilization, the CO₂ plume expands much further into the reservoir than in case of high ED and EV . The plume is more difficult to control and might spread into areas of the reservoir that are not well characterized. On the other hand, a low ϕ_U means a larger fraction of remaining water in proximity to the CO₂ phase. This proximity facilitates secondary trapping processes and therefore leads to faster sequestration of the free CO₂ phase.

Redistribution and Trapping Processes: The primary displacement processes as discussed so far are setting the scene for later processes leading to a redistribution and to trapping of CO₂ in the reservoir. In the post-injection period, the plume still migrates due to gravity differences, which is illustrated in Fig. 5. During secondary migration, the plume might disconnect from the injection well, if there is no CO₂ supply any more. At this point, water starts to imbibe, i.e. to displace CO₂, and since water tends to wet the rock's internal surface, it disconnects the CO₂ phase on the pore scale which forms clusters and bubbles [Iglauer, 2010; Georgiadis, 2013]. This so-called capillary trapping is the first trapping mechanism that kicks in after the stratigraphic trapping.

CO₂ and brine are mutually soluble, but depending on distances and contact areas, dissolution may act over long time scales. The dispersed CO₂ phase partly dissolves in the brine phase and since CO₂-saturated brine has a higher density than fresh brine, it sinks in dissolved form towards the bottom of the reservoir, while the fresh brine is moving upward, eventually contacting the CO₂ plume. This induces brine convection cycles that effectively distribute and immobilize the CO₂ and remove it from the seal (see e.g. [Neufeld, 2010]).

Dissolved CO₂ forms carbonic acid, reacting with the rock-forming minerals. It is generally assumed that subsequent reactions with the formation rock (rock-fluid system) form new solids. This is called mineral trapping and is the ultimate form of trapping since CO₂ turns into rock matrix. Although the time scale and magnitude of mineral trapping is poorly understood and difficult to determine in the lab these processes are known and require very long time scales.

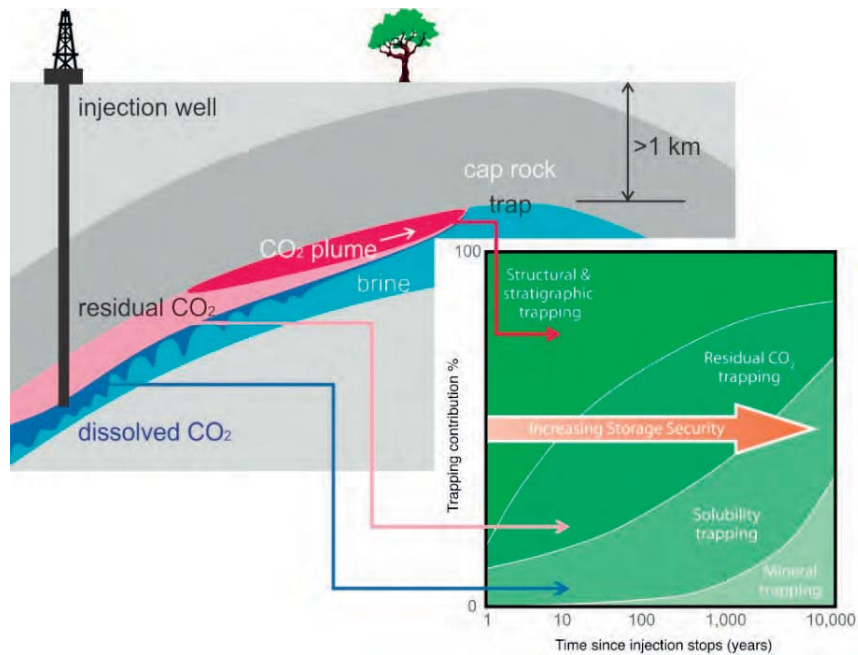


Figure 5: Sketch of secondary plume migration in an anticline structure after injection has stopped. CO₂ is in different states: as connected (plume) and disconnected (residual CO₂) supercritical phase, and dissolved in the brine phase. The arrows connect the schematic with the CO₂ fate plot from [IPCC, 2005], schematically showing the contributions of different trapping mechanisms through time.

The time scales over which the different trapping mechanisms act are schematically shown in the CO₂-fate plot in Fig. 5. However, this is not a universal plot, as the actual time scales depend on many factors such as the capacity and the activity (brine flux) of the aquifer, the reservoir geometry and the exact injection process, which determines the distribution of the CO₂ in the reservoir. The question of how fast and to what extent CO₂ is captured by the formation (dissolved or reacted) and to what extent the CO₂ remains in supercritical phase can be estimated by numerical field simulations of the injection and the post-injection period. How the CO₂-fate plot in Fig. 5 changes for different scenarios has been shown in a case study [Snippe, 2014].

A GLANCE ON CURRENT RESEARCH & DEVELOPMENT

How can we Predict and Observe Plume Migration?

The control of CO₂-plume migration is a classical task of reservoir engineering. With due consideration of a detailed geological description of the reservoir, multiphase-flow physics is applied to predict flow, saturations and distributions of CO₂. In this way, injection operations can be designed by variation of the number and position of injection wells, and of injection rates. Depending on the geology and specific requirements, there are different design criteria. The most evident ones are (1) best confinement of the plume, (2) optimal usage of the pore space – optimization of the storage capacity, and (3) maximum storage safety by e.g. optimizing capillary trapping or maximizing CO₂ dissolution in the brine.

Modelling multi-phase flow on a field scale requires an effective description of fluid mobility and saturations as function of space and time. An effective description is given by the extended Darcy's law (see Nutshell A), which is a phenomenological description that has successfully been applied to oil and gas production over the last decades [Lake, 1989].

Nutshell A: Multiphase flow and extended Darcy's law

Single-phase flow in porous media is described by Darcy's law [Bear, 1972]: (A1) $\vec{v} = -K/\mu \cdot \nabla P$, where K is the absolute permeability of the formation rock, μ the fluid viscosity and \vec{v} the flux. The flux links to the interstitial fluid velocity through v/ϕ , with ϕ being the porosity.

When considering immiscible displacement such as the displacement of brine by CO_2 , both immiscible fluid phases flow simultaneously through the pore space, reducing each other's mobility, i.e. the effective fluid phase permeability. This is described in a phenomenological way by relative permeability saturation functions $k_r(S_{ij})$. In CO_2 storage operations, relative permeability critically influences the CO_2 saturation in the pore space, the migration of the CO_2 plume, and the residually trapped volume after re-imbibition of the aquifer. In numerical models, two-phase flow is described by the following equations – for simplicity we assume incompressible flow without mass transfer between the fluid phases [Bear, 1972; Lake, 1989]:

$$(A2) \quad \phi \frac{\partial S_i}{\partial t} + \nabla \vec{v}_i = 0 \quad \text{and} \quad (A3) \quad \vec{v}_i = -\frac{k_{r,i}K}{\mu_i} (\nabla P_i - \rho_i \vec{g}),$$

where the wetting-phase ($i = w$) and the non-wetting-phase ($i = nw$) saturations satisfy $S_w + S_{nw} = 1$. Eq. A2 is the mass balance equation. The flux \vec{v}_i is described by Darcy's law extended to two-phase flow in Eq. A3, with the fluid phase viscosities and densities μ_i and ρ_i and the gravity constant \vec{g} . The fluid phase mobility is now expressed as $m_i = k_{r,i}K/\mu_i$.

As consequence of preferential wetting of the fluid phases to the rock-forming minerals, the fluid-fluid interfaces are curved in the pore space. This results in a higher pressure in the non-wetting phase than in the wetting, i.e. $P_{nw} > P_w$. This is known as the capillary pressure $p_c = P_{nw} - P_w$. The average interfacial curvature is a function of water saturation, and hence $p_c = p_c(S_w)$.

Relative permeability and capillary pressure functions are typically derived from core flood experiments. Fig. A1 shows a time series of 3D CO_2 -saturation profiles derived from computerized tomography scans of a CO_2 -brine displacement experiment [Berg, 2013]. Relative permeability functions are derived from numerical history matching of saturation profiles, fluid production curve and differential fluid pressures. Such data are directly used in reservoir simulations to predict displacements on the reservoir scale.

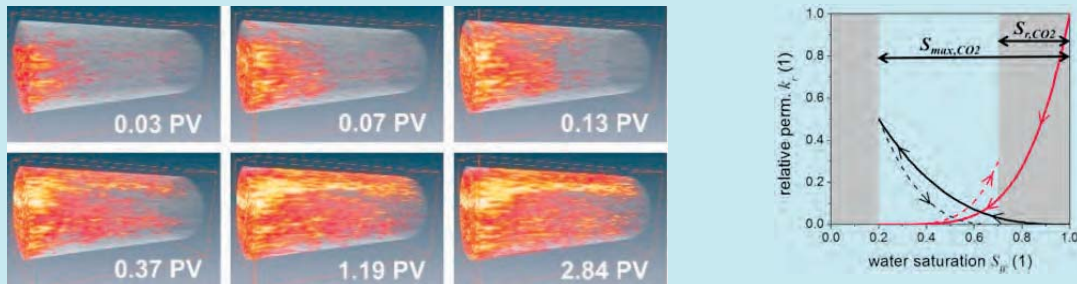


Figure A1: 3D- CO_2 -saturation profiles recorded by means of computerized tomography during a CO_2 -brine displacement experiment in sandstone [Berg, 2013]. CO_2 saturation is displayed in orange/red and the initial brine-saturated rock as semi-transparent background. PV denotes the injected CO_2 volume in units of the total pore volume (PV) of the rock sample. Right: drainage (solid lines) and imbibition (dashed lines) relative permeability curves. The water branches are in red and the CO_2 branches are in black.

The precondition is a profound knowledge of the geological setting of the particular reservoir, which is used as basis for a grid-based static geological model including detailed information on rock properties, heterogeneity etc. Geophysical (e.g. seismic) and petrophysical (well bore logging) data are used to populate the model. Relevant petrophysical data are the rock's porosity, permeability and fluid phase saturation (in case of depleted hydrocarbon fields) as well as fluid phase properties.

The injection process is then modelled on the static geological model. CO_2 -brine displacement (in case of saline aquifers) is subject to two-phase flow (in general to multi-phase flow as in case of CO_2 storage in depleted hydrocarbon fields and during CO_2 -EOR operations). To describe multi-phase flow properties relative phase mobilities must be assigned to each rock formation, which is in general a function of CO_2 saturation. The respective relative-

permeability, $k_r(S_W)$, and capillary-pressure saturation functions, $p_C(S_W)$, can be measured in the laboratory. In modern injection experiments, fluid saturation, i.e. fluid displacements, are monitored by computerized tomography, the differential pressure is measured and the effluent fluids are analyzed [Berg, 2013; Krevor, 2012; Benson, 2013; Ott, 2015]. With this set of information, the experiment can be matched by numerical simulations (history match) in order to derive $k_r(S_W)$ and $p_C(S_W)$ that can directly be used to simulate the CO₂ plume migration on the field scale. Matching the actually observed pressure response (and other parameters) during field operations to reservoir simulations allows the refinement of static reservoir models in an iterative process (history match).

Also a direct observation of plume migration in the field is possible as demonstrated within the Sleipner field operation by Statoil [Chadwick, 2010]. With 4D seismic, changes of acoustic properties induced by CO₂ saturation are observed and tracked over time. Thus plume extent and migration can be monitored and the data can be used to refine the static geological model and the rock-fluid properties during the operation.

Nutshell B: Viscous displacement stability

Supercritical CO₂ has a viscosity which is generally lower than that of the brine, which potentially results in an unstable CO₂ flood front. The necessary condition for unstable displacement is that the displacing fluid has a higher mobility than the displaced fluid ($m_{CO_2} > m_{brine}$). The reason for the instability is that the pressure gradient in a disturbance ahead of the flood front is larger than at the flood front. This is a result of the higher mobility of the displacing fluid phase, which lets the finger grow as shown by the analytical model by [van Wunnik, 1989]. Viscous fingering results in a displacement pattern as schematically shown in Fig. 4.

The phenomenon has been observed in miscible and immiscible displacements [Homsy, 1987]. In contrast to the miscible case where the fluid mobility is given by its viscosity only, $m_i = 1/\mu_i$, the fluid mobility in immiscible displacement is determined by viscosity *and* relative permeability, $m_i = k_{r,i}/\mu_i$. In other words, relative permeability might stabilize the flood front. Miscible and immiscible fingering also differ by the counteracting mechanism to the viscous-driven instability. For miscible situations it is hydrodynamic dispersion that homogenizes concentration or saturation gradients caused by the fingering, whereas for immiscible displacement it is the capillarity dispersion that opposes fingering.

From these stability considerations, the following criteria for the onset of viscous fingering in immiscible displacement can be derived [Berg, 2012]:

$$(B1) \quad M_{SF} = \frac{k_{r,CO_2(shock)}/\mu_{CO_2}}{k_{r,brine(S_W=1)}/\mu_{brine}} > 1 \quad \text{and} \quad (B2) \quad N_{cap}^{macro} = \frac{\mu_{CO_2} v_{CO_2} L}{\overline{p_C} K} > 1,$$

where M_{SF} denotes the shock-front mobility ratio and N_{cap}^{macro} the macroscopic capillary number comparing viscous and capillary forces during displacement. In Eq. B2, L is a characteristic length scale over which capillary pressure disperses the flood front. Such stability criteria can be used for an upfront risk evaluation before starting extensive modeling studies.

So far we have discussed a standard reservoir engineering workflow as applied to oil and gas production operations. However, there are differences between CO₂ storage and standard oil- and gas-production operations due to the combination of rock and fluid properties as outlined above: the low viscosity might lead to channeling in heterogeneous rock structures and potentially to a viscous-unstable flood front. The mutual solubility with water leads to formation drying and eventually to scaling near the injection well. Dissolved CO₂ i.e. carbonic acid dissolves rock-forming minerals, leading to changes in the fluid-flow field and to changes of mechanical rock properties. The couplings of fluid flow, chemical rock fluid interaction, fluid phase properties, and mechanical rock properties are not well understood and are difficult to include in numerical reservoir modeling. A couple of resulting consequences are discussed in the flowing sections and Nutshells.

Nutshell C: Capillary-driven solute transport and salt precipitation

The injected CO₂ is usually under-saturated with respect to water and slowly dissolves formation water around the injection well. The concentration of solutes in the remaining aqueous phase increases and salt precipitates after reaching the solubility limit. The precipitate reduces the pore space around the injection well and eventually the permeability, which might impair injectivity.

In contrast to most hydrogeological problems, where flow is driven by viscous forces, in the drying regime brine saturations (S_w) are generally low and the brine phase is bound by capillary forces and hence is largely immobile. In this regime, flow and solute transport is determined by capillary- and osmotic-driven processes. Drying leads to capillary-pressure gradients that are responsible for macroscopic solute transport, which determines the macroscopic distribution of deposits, and hence the final porosity profile $\phi(x)$ around the injector [Giorgis, 2007; Ott, 2015b]. A counter-current flow of brine induced by a gradient of drying rates in particular might transport large amounts of solutes in the direction towards the injection point where the salt eventually precipitates.

Macroscopic solute transport and the resulting $\phi(x)$ might be modeled on the continuum scale [Pruess, 2009], while on the other hand the associated permeability reduction depends on the exact position of salt crystallization in the pore space. Hence the $K(\phi)$ relationship is of microscopic origin and is determined by microscopic solute transport and eventually the exact microscopic distribution of the precipitate in the pore space [Ott, 2014; Shokri, 2014].

It has been found that heterogeneity in the microscopic rock texture plays a fundamental role in controlling the water evaporation rate and the exact location of deposition [Lehmann, 2009], and that the permeability of different pore systems responds qualitatively different to salt precipitation [Ott, 2014]. The effect of precipitation on the effective permeability ($K_{eff} = Kk_{r,CO_2}$) mainly depends on the presence of microscopic solute-transport mechanisms into the CO₂-conducting flow channels.

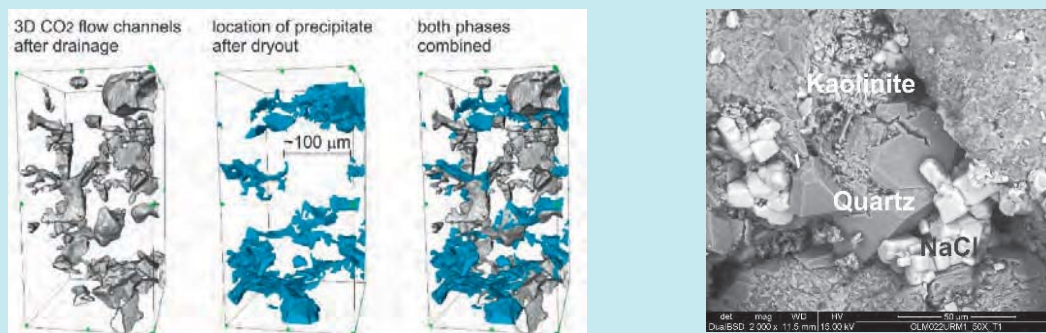


Figure C1: Left: CO₂ flow channel after drainage and the precipitate after dryout of a sandstone rock. The early CO₂ phase and the late precipitate occupy complementary pore space and K_{eff} is unaffected by precipitation [Ott, 2014]. Right: SEM image showing the different mineral phases after the experiment.

Pressure Response and Well-Bore Integrity

In oil and gas production operations, there is usually a net removal of fluids from the reservoir and hence reservoir pressure usually decreases or is maintained. In pure injection operations, reservoir fluids need to be displaced and pressure can be expected to increase – at least temporarily – to above the initial reservoir pressure. The largest pressure increase is usually observed at the injection well. The subsequent pressure decay depends on the detailed architecture of the reservoir and in the simplest case on the total reservoir volume, the reservoir permeability and on the boundary conditions, i.e. whether the reservoir is closed or connected to an open and active aquifer.

The higher the injection pressure, the higher is the pressure exerted on the sealing cap rock, which increases the risk of seal failure. Normally, highly permeable formations are considered a target for CO₂ storage, for which the injection pressure stays well below the entry pressure

and the fracturing pressure of the cap rock. For a given formation permeability, the injection pressure mainly depends on the injection rate and its evolution is predicted by numerical simulations and monitored during the operation. However, there are threats. The injected CO₂ is usually not in chemical equilibrium with the rock formation and the resident fluid. Water dissolves in the CO₂ phase, which causes the salts originally dissolved in the brine to precipitate.

Precipitation reduces the rock's pore space and permeability. The degree of permeability reduction has been found to depend on the exact pore structures of the rock and can range to several orders of magnitude, which bears comparison with losing injectivity and eventually the well (Nutshell C).

On the other hand, as has been mentioned, CO₂ forms carbonic acid in water-bearing formations, leading to dissolution of rock-forming minerals, possibly also to mineral precipitation. The consequences of mineral dissolution are not easy to predict. Depending on the specific reactive-transport regime, different dissolution patterns occur with different implications for operations: (1) a rather uniform change of the flow field and potential subsidence of the formation if dissolution is homogeneous and ranging deep into the

Nutshell D: Reactive transport and dissolution regimes

The injected CO₂ forms carbonic acid in water-bearing reservoir rocks, which causes mineral-dissolution and precipitation reactions. For the injection of acid solutions, dissolution regimes are characterized by Péclet (Pe) and Damköhler (Da) numbers, being the ratios of advective to diffusive transport rates, $Pe = ul/D$, with u being the fluid velocity, l representing length scale of the pore system, and D being the diffusion coefficient, and the ratio of the overall dissolution rate to the advective transport rate, $Da = kl/u$, with k being the overall reaction rate [see e.g. Golfier, 2002].

At low reaction rates, slow and spatially homogeneous dissolution is expected, changing the flow and mechanical rock properties over longer time scales in a homogeneous way. If the rate of reaction is fast compared to typical transport rates, and dissolution is more localized, a dissolution fronts appears. At high Pe and Da numbers, such dissolution fronts can be unstable, leading to the formation of highly conductive flow channels, i.e. wormholes. However, the situation is more complex for CO₂ injection operations than for injection of acidic solutions in the case of well stimulation operations since CO₂ does not directly react with rock-forming minerals but acts as acid-forming agent. Hence single-phase non-reactive (e.g. ahead of the CO₂ front) and two-phase flow reactive transport domains are expected. The consequences are not yet well understood, but it has been shown that Pe and Da numbers alone are not sufficient to describe dissolution regimes in two-phase flow, and that the capillarity of the evolving dissolution structure must be taken into account [Ott, 2015c].

The implementation of reactive transport in reservoir modeling remains a challenge. While sufficiently homogeneous dissolution can already be modeled reliably, localized dissolution structures are typically beyond the resolution of field-scale modeling. The implementation of local structure formation and the upscaling to effective flow and mechanical properties on the continuum scale is currently an active field in R&D.



Figure D1: Detailed view on dissolution patterns as result of carbonic-acid injection and the co-injection of CO₂ and brine (right). At the same brine injection rate (i.e. the same Pe and Da numbers) we find wormhole formation in single-phase flow and a rather compact dissolution front in two-phase flow [Ott2015c].

reservoir, (2) a compact dissolution front would not affect the formation properties, but the mechanical integrity of the rock at the well casing, causing well bore stability issues, and (3) improved injectivity and directional flow due to the formation of wormholes (unstable dissolution front). The latter two regimes mainly occur in carbonate fields. Wormhole formation improves injectivity and might lead to directional (channeled) flow of injected fluids. Flow regimes are briefly discussed in Nutshell D.

Long Term Storage Security

The mobility of the CO₂-rich phase is a key aspect for the evaluation of the storage security. After termination of the injection, during secondary plume migration, water imbibes in the CO₂-saturated reservoir volumes. Typically, the mobility of fluid phases are manifested in relative fluid permeability $k_r(S_w)$ as determined in imbibition core flood experiments and as used for oil and gas production modeling. However, in CO₂ storage time scales in the order of millennia are relevant for safe storage, i.e. measurements with the purpose of resolving the time scales relevant for oil and gas fields may not be sufficient.

During the imbibition process, the CO₂ phase becomes disconnected into clusters, leading to capillary trapping of CO₂. The mobility of the CO₂ phase is then governed by the microscopic

Nutshell E: Mobilization of non-wetting fluid clusters:

During an imbibition process, the initially connected non-wetting phase breaks up in disconnected ganglia or clusters (snap off). The size of the clusters determines their mobility, since a large cluster experiences a larger viscous-track force due to wetting-phase flow than a small cluster and hence can overcome the capillary barrier that holds the cluster in place. The interplay between the viscous-track force and capillary forces is expressed in the macroscopic capillary number [Hilfer, 1996; Armstrong, 2014]

$$(E1) \quad N_{cap}^{macro} = \frac{\mu_w v_w l_{cl}}{p_c K_w}$$

(see Nutshell B). In contrast to Eq. B2, the velocity, viscosity and permeability refer to the wetting phase, and the length scale refers to the cluster length, which is rather of mesoscopic scale.

Recent developments in pore-scale imaging and modeling allow the visualization of clusters and the determination of their morphology and sizes. Cluster size distributions [Iglauer, 2010; Georgiadis, 2013] and average curvatures of fluid-fluid interfaces [Armstrong, 2014; Andrew, 2014] and their distributions as well as in-situ contact angles of fluids to rock [Andrew, 2014] can be derived to better characterize macroscopic flow properties. Such data allow to determine the structure and mobility of a trapped CO₂ phase more accurately than in macroscopic relative-permeability measurements, and allow insight in the displacement mechanisms. Recently, time-resolved pore-scale imaging has been used to identify mechanisms of ganglion dynamics beyond the viscous-track force through break-up and coalescence of clusters [Rücker, 2015].

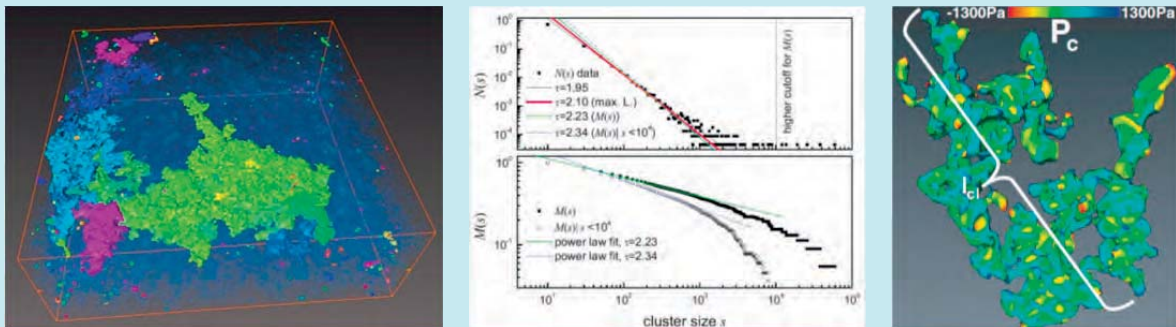


Figure E1: Non-wetting phase clusters in a porous media (left) and cluster size distribution (middle) after shut in [Georgiadis, 2013]. Right: topology of a non-wetting phase cluster. The color code denotes the interfacial curvature scaled to capillary pressure [Armstrong, 2014].

topology of these fluid clusters: the clusters, their size, and cluster-size distributions are fundamental for predicting the efficiency of capillary trapping. It has earlier been suggested that the balance between viscous and capillary forces – the capillary number – governs the mobilization of non-wetting fluid clusters. With recent advances in pore-scale imaging and modeling it became feasible to investigate cluster size distributions, cluster topology and mobility on the microscopic scale. The obtained statistical data help to evaluate the overall mobility of “trapped” CO₂ phases and the criteria for phase mobilization and trapping. Pore-scale data can be used to design injection projects in order to optimize the balance between storage capacity and long-term storage security (see Nutshell E).

After this first phase where, even as clusters, supercritical CO₂ is in principle still mobile, with a tendency to migrate upwards, the next level of security is reached as CO₂ dissolved in the formation brine and/or forms a mineral phase that can be considered as permanently trapped. The limiting step of the overall dissolution rate is considered to depend on the macroscopic transport rates of fresh and CO₂-saturated brine to and from the scCO₂ saturated regions in the reservoir. These macroscopic transport processes essentially depend on the solubility limits of CO₂ in brine, the gravity difference between fresh and CO₂-saturated brine, and on plume and reservoir geometry. The gravity difference results in convection cycles in the field, which can be modeled on the reservoir scale. Again, chemical reactions might add some uncertainty with respect to the permeability field, which eventually influences the time scale of dissolution trapping and the spatial distribution of dissolved CO₂ [Ennis-King, 2007].

Estimation of Storage Capacity

An assessment of the CO₂ storage potential requires the estimation of the storage capacity on a global and regional scale in relation to the locations, emission rates, and lifetimes of CO₂-emitting plants. As for the estimation of accessible hydrocarbon accumulations, the concept of resources and reserves can be used to assess CO₂ storage capacity [Bradshaw, 2007; Bachu, 2007]. Resources are those quantities of commodities that are estimated to exist on the considered scale. Reserves are those that are known to exist and that are feasible under current technological and economic conditions. The total resources would be equivalent to the total pore space available in a basin or field that can permanently hold CO₂ in its pure phase – this is the volumetric limit of what a geological system can accept and it is called the theoretical storage capacity (TSC). The TSC represents the upper limit of the capacity estimation.

By taking the technical (geological and engineering) cut-off limits into account, we arrive at a lower and more realistic value, which is the effective storage capacity (ESC). Limits are the efficiency of fluid-displacement processes and natural limits of injection pressure discussed above. The viable storage capacity (VSC) is a the fraction of the ESC that considers not only the technical aspects, but also the legal and regulatory demands, as well as the available infrastructure and other economic barriers to CO₂ geological storage. Finally, a detailed matching of large stationary CO₂ sources with the geological storage sites further reduces the storage space. Practically, eventually only a small fraction of the total pore space can be utilized for subsurface storage.

Ignoring legal and economic aspects, we focus here on ESC which is the fraction of the total reservoir pore volume that is technically feasible for CO₂ storage. It depends on the type of reservoir, the type of operation, the intended storage mechanism and the thermodynamic conditions expected in the field.

For storage in depleted hydrocarbon fields the capacity can be estimated under the assumption that the volume previously occupied by the produced hydrocarbons is available for CO₂ storage. The mass of CO₂ that can be sequestered in such a field corresponds to the volume of

produced hydrocarbons (at initial reservoir pressure and temperature conditions) multiplied by the density of CO₂ under the same initial reservoir conditions. This is a valid assumption for pressure-depleted reservoirs that are not in hydrodynamic contact with an aquifer and not flooded for secondary or tertiary oil recovery. If the reservoir is water-flooded, it is likely that not all the previously occupied pore space can be used for storage. The previously discussed concepts of displacement and sweep efficiency and the limitation of injection pressure must be taken into account to determine the pore-space utilization.

The ESC in deep saline aquifers mainly depend on the intended predominant trapping mechanism. The TSC in a stratigraphic trap is similar to the depleted field case. It is the total pore volume of the stratigraphic trap down to the spill point, reduced by the irreducible water saturation that limits the pore space. The respective ESC takes the displacement and sweep efficiency at a given injection configuration into account, as well as the limitation in injection pressure, which has to be higher than the initial water pressure to displace the brine phase, and lower than the threshold entry pressure of the CO₂ in the cap rock and lower than the fracturing pressure. The maximum injection pressure limits the phase density of CO₂ and the displacement process – both limiting the storage density.

If the predominant storage mechanism is residual trapping, as in case of hydrodynamic trapping [Bachu, 1994], the ESC is based on the CO₂ migration path (after injection has stopped) and the residual gas saturation (instead of residual water saturation as in case of stratigraphic trapping). The storage density is generally much lower and the migration distance larger than in case of stratigraphic trapping. As far as solubility trapping is concerned, ESC is limited by the CO₂-solubility limit in brine, and time scales of dissolution are determined by the density difference between fresh and CO₂-saturated brine and the respective gravity-driven transport. However, solubility trapping is a secondary effect that rather depends on the aspects of reservoir geometry and CO₂ plume migration (which rather should be considered for capacity estimation).

A standardized methodology to estimate storage capacities as developed by Bachu and Bradshaw and discussed above has been applied in many regions of the world. The literature has been summarized by Dooley [Dooley, 2013] who reported that the global effective storage capacity (ESC) could be as large as 13500 Gt CO₂. Despite the uncertainties, Dooley concludes that a lack of geologic storage space is unlikely to be the primary impediment to CCS deployment as the average demand for geologic CO₂ storage ranges from 448 to 1000 Gt CO₂ [Dooley, 2013; IPCC, 2014].

SUMMARY AND CONCLUSIONS

Geological carbon storage is an essential part in the CCS technology chain and a key technology to mitigate CO₂ emissions from anthropogenic sources. In combination with bioenergy, CCS (or BECCS) even has the potential to enable a negative emission footprint, i.e. with BECCS actively removing carbon from the atmosphere and from the surface (short-term) carbon cycle.

The pivotal question is whether or not geological CO₂ storage is safe, effective, and affordable. Natural analogs demonstrate that CO₂ can be stored over millions of years. However, as with other technologies, geological carbon storage bears some risks, which can be controlled when applied with care. First of all, the principles of carbon storage are essentially explored and the storage processes can reliably be modelled. In particular, depleted gas fields and sandstone reservoirs are promising candidates for storage operations, while current R&D is focused on carbonate reservoirs. Those are more complex due to their multi-

scale structural heterogeneities. Also the high reaction rates of carbonates with carbonic acid raises some challenges for predictive modeling.

Despite the challenges and ongoing R&D, current knowledge and capabilities are sufficient to already identify safe subsurface containers in which CO₂ can safely be stored. But even in such cases, an elaborate effort of reservoir characterization and reservoir engineering is needed to guarantee safe storage and to optimize injection performance and storage capacity.

REFERENCES

- [Andrew, 2014] Andrew, M., Bijeljic, B., and Blunt, M. J. (2014). Pore-scale imaging of trapped supercritical carbon dioxide in sandstones and carbonates. *International Journal of Greenhouse Gas Control*, 22:1–14.
- [Armstrong, 2014] Armstrong, R., Georgiadis, A., Ott, H., Klemin, D., and Berg, S. (2014). Critical capillary number: Desaturation studied with fast X-ray computed microtomography. *Geophys. Res. Lett.*, 41:1–6.
- [Bachu,1994] Bachu, S., Gunter, W. D., and Perkins, E. H. (1994). Aquifer disposal of CO₂: Hydrodynamic and mineral trapping. *Energy Convers. Mgmt.*, 34:487–496.
- [Bachu, 2007] Bachu, S., Bonijoly, D., Bradshaw, J., Burruss, R., Holloway, S., Christensen, N. P., Mathiassen, O. M. (2007). CO₂ storage capacity estimation: Methodology and gaps. *International Journal of Greenhouse Control*, 1:430–443.
- [Bear, 1972] Bear, J. (1972). *Dynamics of Fluids in Porous Media*. Elsevier.
- [Benson, 2013] Benson, S., Pini, R., Reynolds, C., and Krevor, S. (2013). Relative permeability analysis to describe multi-phase flow in CO₂ storage reservoirs (no. 2). Global CCS Institute.
- [Benson, 2014] Benson, S. (2014). Negative-emissions insurance. *Science*, 344:1431.
- [Berg, 2012] Berg, S. and Ott, H. (2012). Stability of CO₂-brine immiscible displacement. *International Journal of Greenhouse Control*, 11:188–203.
- [Berg, 2013] Berg, S., Oedai, S., and Ott, H. (2013). Displacement and mass transfer between saturated and unsaturated CO₂-brine systems in sandstone. *International Journal of Greenhouse Gas Control*, 12:478–492.
- [Bradshaw, 2007] Bradshaw, J., Bachu, S., Bonijoly, D., Burruss, R., Holloway, S., Christensen, N. P., Mathiassen, O. M. (2007). CO₂ storage capacity estimation: Issues and development of standards. *International Journal of Greenhouse Control*, 1:62–68.
- [Buckley and Leverett, 1942] Buckley, S. E. and Leverett, M. C. (1942). Mechanism of fluid displacement in sands. *Transactions of the AIME*, 146:107–116.
- [Busch, 2011] Busch, A. and Gensterblum, Y. (2011). CBM and CO₂-ECBM related sorption processes in coal: A review. *International Journal of Coal Geology*, 87(2): 49-71.
- [Chadwick, 2010] Chadwick, A., Williams, G., Delepine, N., Clochard, V., Labat, K., Sturton, S., Buddensiek, M.-L., Dillen, M., Nickel, M., Lima, A. L., Arts, R., Neele, F., and Rossi, G. (2010). Quantitative analysis of time-lapse seismic monitoring data at the Sleipner CO₂ storage operation. *The Leading Edge*, 29(2):170-177.
- [Dooley, 2013] Dooley J. J. (2013). Estimating the supply and demand for deep geologic CO₂ storage capacity over the course of the 21st Century: A meta analysis of the literature. *Energy Procedia* 37, 5141 – 5150.

- [EIA, 2014] US Energy Information Administration (2014). International energy statistics – www.eia.gov.
- [Ennis-King, 2007] Ennis-King, J., and Paterson, L. (2007). Coupling of geochemical reactions and convective mixing in the long-term geological storage of carbon dioxide. *International Journal of Greenhouse Gas Control*, 1:86–93.
- [Georgiadis, 2013] Georgiadis, A., Berg, S., Maitland, G., and Ott, H. (2013). Porescale micro-computed-tomography imaging: Nonwetting-phase cluster-size distribution during drainage and imbibition. *Phys. Rev. E*, 88(3):033002–033011.
- [Giorgis, 2007] Giorgis, T., Carpita, M., and Battistelli, A. (2007). 2D modeling of salt precipitation during the injection of dry CO₂ in a depleted gas reservoir. *Energy Conversion and Management*, 48:1816–1826.
- [Global CCS Institute, 2015] Global CCS Institute (2015). CCS project data base, www.globalccsinstitute.com.
- [Golfier, 2002] Golfier, F., Zarcone, C., Bazin, B., Lenormand, R., Lasseux, D., and Quintard, M. (2002). On the ability of a Darcy-scale model to capture wormhole formation during the dissolution of a porous medium. *J. Fluid Mech.*, 457:213–254.
- [Hilfer, 1996] Hilfer, R. and Øren, P. E. (1996). Dimensional analysis of pore scale and field scale immiscible displacement. *Transport in Porous Media*, 22:53–72.
- [Homsy, 1987] Homsy, G. M. (1987). Viscous fingering in porous media. *Annual Review of Fluid Mechanics*, 19:271.
- [IEA, 2014] International Energy Agency (2014). Key world energy statistics.
- [Iglauer, 2010] Iglauer, S., Favretto, S., Spinelli, G., Schena, G., and Blunt, M. (2010). X-ray tomography measurements of power-law cluster size distributions for the nonwetting phase in sandstones. *Physical Review E*, 82(5):056315–1–056315–3.
- [IPCC, 2005] IPCC (2005). IPCC Special Report on Carbon Dioxide Capture and Storage. Cambridge University Press, UK.
- [IPCC, 2014] IPCC (2014). Working Group III Contribution to the Fifth Assessment Report of the Intergovernmental Panel on Climate Change. Cambridge University Press, UK.
- [Krevor, 2012] Krevor, S. C. M., Pini, R., Zuo, L., and Benson, S. M. (2012). Relative permeability and trapping of CO₂ and water in sandstone rocks at reservoir conditions. *Water Resour. Res.*, 48:W02532.
- [Lake, 1989] Lake, L. W. (1989). *Enhanced Oil Recovery*. Prentice Hall.
- [Lehmann, 2009] Lehmann, P. and Or, D. (2009). Evaporation and capillary coupling across vertical textural contrasts in porous media. *Phys. Rev. E*, 80:046318.
- [McGlade, 2015] McGlade, C. and Ekins, P. (2015). The geographical distribution of fossil fuels unused when limiting global warming to 2°C. *Nature*, 517:187–190.
- [Meinshausen, 2009] Meinshausen, M., Meinshausen, N., Hare, W., Raper, S. C. B., Frieler, K., Knutti, R., Frame, D. J., and Allen, M. R. (2009). Greenhouse-gas emission targets for limiting global warming to 2°C. *Nature*, 458:1158–1162.
- [MIT, 2015] MIT (2015). Carbon capture and sequestration technologies program, <http://sequestration.mit.edu>.

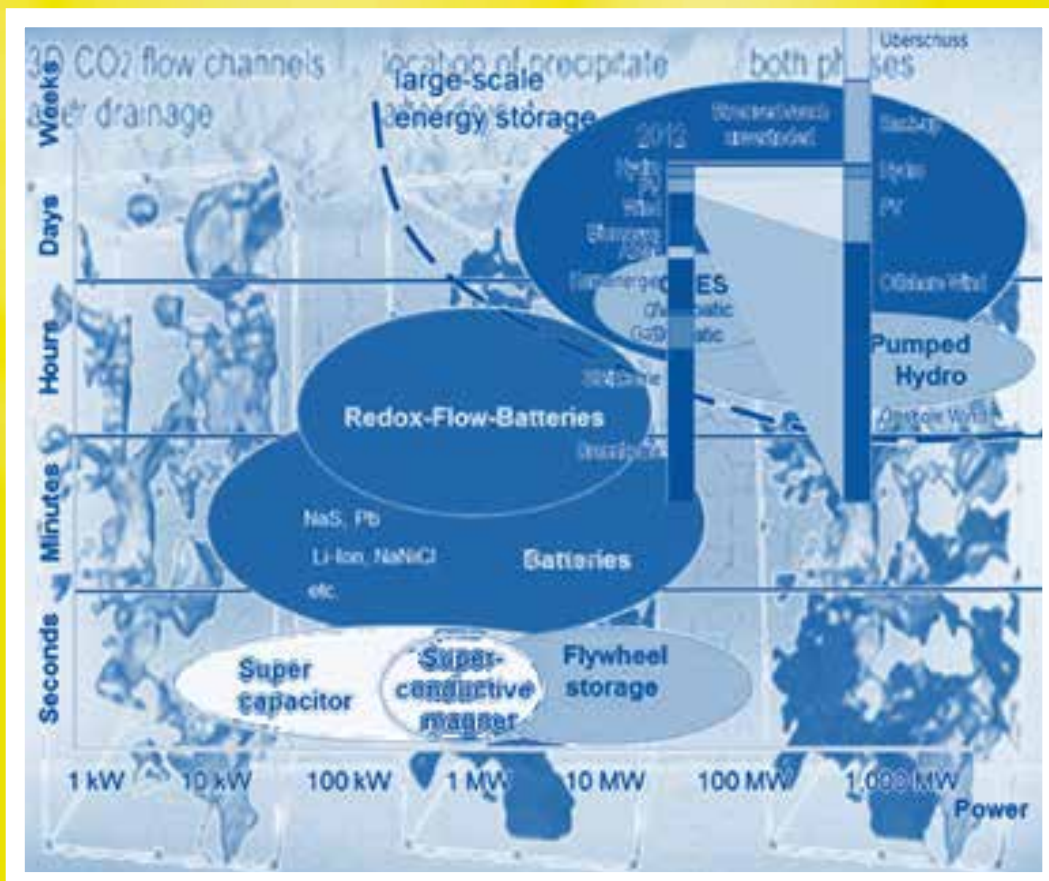
- [Neufeld, 2010] Neufeld, J. A., Hesse, M. A., Riaz, A., Hallworth, M. A., Tchelepi, H. A., and Huppert, H. E. (2010). Convective dissolution of carbon dioxide in saline aquifers. *Geophysical Research Letters* 37, L22404.
- [Ott, 2014] Ott, H., Andrew, M., Snippe, J., and Blunt, M. (2014a). Microscale solute transport and precipitation in complex rock during drying. *Geophysical Research Letters*, 41(23):8369–8376.
- [Ott, 2015] Ott, H., Pentland, C. H., and Oedai, S. (2015). CO₂-brine displacement in heterogeneous carbonates. *International Journal of Greenhouse Control*, 33:135–144.
- [Ott, 2015b] Ott, H., Roels, S., and de Kloe, K. (2015b). Salt precipitation due to supercritical gas injection: I. capillary-driven flow in unimodal sandstone. *International Journal of Greenhouse Gas Control*, online: doi:10.1016/j.ijggc.2015.01.005.
- [Ott, 2015c] Ott, H. and Oedai, S. (2015). Wormhole formation and compact dissolution in single- and two-phase CO₂-brine injections. *Geophysical Research Letters*, online, doi: 10.1002/2015GL063582.
- [Pruess, 2009] Pruess, K. and Müller, N. (2009). Formation dry-out from CO₂ injection into saline aquifers: 1. effects of solids precipitation and their mitigation. *Water Resour. Res.*, 45:W03402.
- [Raupach, 2014] Raupach, M. R., Davis, S. J., Peters, G. P., Andrew, P. M., Canadell, J. G., Ciais, P., Friedlingstein, P., Jotzo, F., van Vuuren, D. P., and Le Quéré, C. (2014). Sharing a quota on cumulative carbon emissions. *Nature Climate Change*, 4:873–879.
- [Rücker, 2015] Rücker, M., Berg, S., Armstrong, R. T., Georgiadis, A., Ott, H., Schwing, A., Neiteler, R., Brussee, N., Makurat, A., Leu, L., Wolf, M., Khan, F., Enzmann, F., Kersten, M. (2015). From Connected Pathway Flow to Ganglion Dynamics. *Geophysical Research Letters*, online, doi: 10.1002/2015GL064007.
- [Shell, 2013] Shell (2013). Royal Dutch Shell plc: Sustainability report 2013.
- [Shokri, 2014] Shokri, N. (2014). Pore-scale dynamics of salt transport and distribution in drying porous media. *Physics of Fluids*, 26:012106.
- [Snippe, 2014] Snippe, J. and Tucker, O. (2014). CO₂ fate comparison for depleted gas field and dipping saline aquifer. *Energy Procedia*, 63:5586–5601.
- [van Vuren, 2011] van Vuuren, D. P., Edmonds, J., Kainuma, M., Riahi, K., Thomson, A., Hibbard, K., Hurtt, G. C., Kram, T., Krey, V., Lamarque, J.-F., Masui, T., Meinshausen, M., Nakicenovic, N., Smith, S. J., Rose, S. K. (2011). The representative concentration pathways: an overview. *Climatic Change* 109:5–31.
- [van Wunnik, 1989] van Wunnik, J. N. M. and Wit, K. (1989). A simple analytical model of the growth of viscous fingers in heterogeneous porous media. In: 1st European Conference on the Mathematics of Oil Recovery. University of Cambridge.

Dr. Holger Ott

Imperial College London, London, SW7 2AZ, United Kingdom

Shell Global Solutions International B.V., 2288 GS Rijswijk, The Netherlands

Exzerpt aus Tagungsband des AKE, DPG-Tagung 2015 Berlin, (ISBN 978-3-9811161-7-5)
home: http://www.uni-saarland.de/fak7/fze/AKE_Archiv/DPG2015-AKE_Berlin/Links_DPG2015.htm
Urquelle: <https://www.dpg-physik.de/veroeffentlichung/ake-tagungsband.html>



Energie

Erzeugung - Netze - Nutzung

Vorträge auf der DPG-Frühjahrstagung in Berlin 2015

Herausgegeben von Hardo Bruhns

Arbeitskreis Energie in der Deutschen Physikalischen Gesellschaft

Direkter Link zum AKE - Archiv:

<http://www.uni-saarland.de/fak7/fze/index.htm>

Direkter Link zum AKE - Archiv, Tagung 2015 -Berlin:

http://www.uni-saarland.de/fak7/fze/AKE_Archiv/DPG2015-AKE_Berlin/Links_DPG2015.htm

Zur Sammlung der Tagungsbände des AKE auf dem DPG - Server:

<https://www.dpg-physik.de/veroeffentlichung/ake-tagungsband.html>

Vorträge auf der Berliner DPG-Tagung (2015)

Herausgeber:
Arbeitskreis Energie (AKE) in der DPG
Prof. Dr. Hardo Bruhns
Meliesallee 5
40597 Düsseldorf
E-Mail: ake@bruhns.info

Die Grafik des Einbandes wurde
mit freundlicher Genehmigung der
Autoren unter Verwendung von
Abbildungen aus den Beiträgen von
H. Milsch, M. Waidhas und F.
Wagner gestaltet.

Energie

Erzeugung - Netze - Nutzung

Vorträge auf der DPG-Frühjahrstagung in Berlin 2015

Arbeitskreis Energie in der Deutschen Physikalischen Gesellschaft

Herausgegeben von Hardo Bruhns

Bad Honnef, September 2015

Frühjahrstagung des Arbeitskreises Energie
in der Deutschen Physikalischen Gesellschaft
Berlin, 16. bis 18. März 2015

Haupt- und Fachvorträge

Inhaltsverzeichnis / Table of Contents

Introduction	7
Fachsitzungen / Sessions	8
Abstracts	9
Organic Photovoltaics: Status and Perspectives - presented by J. Widmer	28
Concepts for Cost Reduction in CSP Power Plants - presented by R. Pitz-Paal	42
Optionen und Trends der Biomassenutzung – Perspektiven für die Bioenergie 2050 - vorgetragen von J. Ponitka	53
Deep Geothermal Fluid Resources: Energetic Use and Beyond - presented by H. Milsch	63
Geological Carbon Storage: Processes, Risks and Opportunities - presented by H. Ott	77
„Fracking“ – Routine oder Risikotechnologie? - vorgetragen von M. Kosinowski	94
Power to Gas – an Economic Approach for Energy Storage? - presented by M. Waidhas	107
Nuclear Fission Energy: New Build, Operation, Fuel Cycle and Decommissioning in the International Perspective - presented by S. Nießen	113

Wendelstein 7-X – Ein Konzept für ein stationäres Fusionsplasma	122
- vorgetragen von R. C. Wolf	
Neue Materialien und Komponenten für energieeffiziente Gebäudehüllen	131
- vorgetragen von U. Heinemann	
Eigenschaften einer Stromversorgung mit intermittierenden Quellen	138
- vorgetragen von F. Wagner	
Transient Stability of Conventional Power Generating Stations during Times of High Wind Penetration	156
- presented by M. Zarifakis	
Ganzheitliche Bewertung von Energiesystemen	168
- vorgetragen von R. Friedrich	
Impressum	183

Der vorliegende Band versammelt schriftliche Ausarbeitungen von Vorträgen auf der Tagung des Arbeitskreises Energie in der Deutschen Physikalischen Gesellschaft des Jahres 2015 in den Räumen der Technischen Universität Berlin. Leider ist es nicht gelungen, von allen Vortragenden Manuskripte zu erhalten. Die Präsentationsfolien der meisten Hauptvorträge können auf der Webseite des Arbeitskreises über:

<http://www.dpg-physik.de/dpg/organisation/fachlich/ake.html>

(von dort gelangt man zum Archiv des AKE) eingesehen werden. Allen, die zu diesem Sammelband beigetragen haben, sei an dieser Stelle sehr herzlich gedankt.